

Classification of natural rubber foam grades by optimising the azodicarbonamide content

Fateehah Baru¹ Sitisaiyidah Saiwari¹ and Nabil Hayeemasae^{1*}

¹*Department of Rubber Technology and Polymer Science, Faculty of Science and Technology, Prince of Songkla University, Pattani Campus, Pattani, Thailand*

*nabil.h@psu.ac.th

Abstract

This study aimed to focus on classifying rubber foam grades according to ASTM D1056. The natural rubber foams were prepared by varying the Azodicarbonamide (ADC) content from 2 - 10 phr. The results were evaluated on their physical and mechanical properties. The relative foam density of the foams decreased, and the expansion ratio increased with the addition of ADC. This was due to the increase in the gas phase raised by ADC. In addition, adding ADC also decreased hardness and compression-deflection of the foams, whereby the values obtained were higher after oven aging due to the radical recombination caused by chain breaking. According to ASTM D1056, the compression-deflection values of the foams were 2A2 and 2A3 grades, where the ADC content at 6 – 10 phr met the basic properties required by the same standard. Furthermore, the ADC content at 6 phr is strongly suggested when considering the foam morphology.

Keywords: azodicarbonamide, compression-deflection, foam, natural rubber.

How to cite: Baru, F., Saiwari, S., & Hayeemasae, N. (2022). Classification of natural rubber foam grades by optimising the azodicarbonamide content. *Polímeros: Ciéncia e Tecnologia*, 32(2), e2022014. <https://doi.org/10.1590/0104-1428.20210111>

1. Introduction

Natural rubber (NR) has been primarily used as a raw material in the production of tyres. Tyre manufacturing consumes 75% of the total global production of NR^[1,2]. The remaining uses of NR vary, and it is utilised in many applications, such as automotive parts, latex gloves, condoms and so forth. Therefore, particular attention is being given to expanding the usage of NR to other industrial products. Natural rubber foam (NRF) is an interesting rubber product that consists of rubber and gas phases in one item. NRF has been used in many applications because of its lightweight, good thermal insulation and sound absorption^[3,4]. There are several methods for producing NRF. Generally, it is produced by the NR latex process, which is in liquid form. The colloidal nature of the latex requires chemical stabilisation (usually obtained with the addition of ammonia). This stabilisation mechanism and the quality of the latex can be affected by the storage time and environment^[5,6]. Alternatively, rubber foams can be produced using the dried rubber process. In this research, dry rubber was used to produce foam because the processing of rubber foam from dry rubber is easier than the process involving latex.

Making NRF from dry rubber is achieved by using an additive called a blowing agent. The foam structure can be controlled by the proper selection of blowing agents and curatives, which achieves the correct balance between the gas generated and the degree of curing. There are many types of chemical blowing agents, such as sodium bicarbonate, p-toluenesulphonyl semicarbazide, 5-phenyl tetrazole, 4,4-oxydibzenesulphonyl hydrazide (OBSH), dinitro

pentamethylene tetramine (DPT) and azodicarbonamide (ADC). Several authors have studied how the content and type of a chemical blowing agent affects elastomers^[7-10]. For example, Pechurai et al.^[8] studied the effect of the foaming agent content on the cell morphology and mechanical properties of NR foams. They observed that increased foaming agent content decreased foam density and hardness due to an increase in cell size. Charoeythornkhajhornchai et al.^[9] reported that the bulk density of NRF significantly decreases and the volumetric expansion ratio of NRF increases when the chemical blowing agent content is high. Coalescence between bubbles was observed in the specimens with 5 and 6 phr of ADC, owing to the high gas content in the rubber matrix. Lee and Choi^[10] studied the effects of foaming temperature and carbon black content on NRF. Their results showed that higher carbon black content increased the density and mechanical properties of the foam, including its tensile strength, tear strength, hardness, modulus and stiffness. Among these, ADC is interesting as a chemical blowing agent because it leads to closed-cell foam and decomposes at low temperatures^[9].

When examining the related documents, it was clear that few studies have addressed the basic properties required by a certain standard, ASTM D1056. Table 1 shows the basic properties required by ASTM D1056. This standard refers to specific properties in order to classify foam grades; for example, it refers to the compression-deflection before and after thermal ageing, as well as the foam's water absorption capacity. This enables a distinction to

Table 1. Basic requirement of cellular rubber (Closed-cell Sponge) according to ASTM D1056.

Grade Number	Compression-Deflection at 25% Deflection (kPa)	Change in compression-deflection after aging at 70°C for 168 h (%)	Water absorption (%)	
			Density over 160 kg/m ³	Density of 160 kg/m ³ or less
2A0	Less than 15	± 30	5	10
2A1	15 – 35	± 30	5	10
2A2	35 – 65	± 30	5	10
2A3	65 – 90	± 30	5	10
2A4	90 – 120	± 30	5	10
2A5	120 – 170	± 30	5	10

Remark: Type 2 is for Closed-cell rubber and Class A is for cellular rubber made from synthetic rubber, natural rubber, reclaimed rubber, or rubber-like materials where a number from 0 – 5 is based on a specific range of firmness as expressed by compression-deflection.

be made between open and closed-cell foams and would help rubber compounders to classify foam grades based on a recognised standard. In this study, NR foams were prepared by varying the concentration of ADC (2, 4, 6, 8 and 10 phr), which was used as the blowing agent, at a fixed processing time and temperature. The impacts of the ADC content on the physical and impact properties of the foams were analysed. The aim of this study was to prepare NRF that meets the basic requirements of the standard specification for flexible cellular materials like sponge or expanded rubber (ASTM D1056). These physical properties include the curing characteristics, relative foam density, compression-deflection before and after ageing and morphology. So far, no reports have focused extensively on the correlations between the basic properties of foams and the ASTM D1056. Besides, this study also introduces a new formulation for preparing the foam. In particular, the use of processing oil and calcium carbonate to promote an even distribution of cellular structure. Processing oil can help to reduce the viscosity to assist the diffusion of gas while the calcium carbonate is widely known to act as a nucleating agent in the production of foam^[11]. The results obtained from this work will be useful for rubber foam manufacturers as a predetermined observation of the preparation of NRF.

2. Experimental methods

2.1 Materials

The NR used in this study was STR 5L, purchased from Suansom Kanyang, Yala, Thailand. ADC was used as the blowing agent and was purchased from A.F. Supercell Co., Ltd., Rayong, Thailand. Treated distillate aromatics extract (TDAE oil) was used as processing oil which was purchased from H&R ChemPharm (Thailand) Co., Ltd. Calcium carbonate (CaCO_3) was obtained from Krungthepchemi Co., Ltd, Bangkok, Thailand. Stearic acid was purchased from Imperial Chemical Co., Ltd., Bangkok, Thailand. ZnO was obtained from Global Chemical Co., Ltd., Samut Prakan, Thailand. Stearic acid and ZnO were used as activator. 2,2,4-trimethyl-1,2-dihydroquinoline (TMQ) and N-cyclohexyl-2-benzo thiazole sulphenamide (CBS) were used as antioxidant and accelerator respectively. These were purchased from Flexsys America L.P., West Virginia, USA and sulfur was purchased from Siam Chemical Co., Ltd., Samut Prakan, Thailand.

2.2 Preparation of natural rubber foam

Table 2 lists the materials used at the start of the process for compounding the NRF. The full amounts of the NR, ADC, TDAE oil and other additives were prepared using a two-roll mill. The compounds were free-blown into specific shapes (12.5 mm in thickness) inside the compression-moulded at the temperature of 150 °C. The time consumed was based on the curing times determined by a moving-die rheometer (MDR), as described in the following section.

2.3 Measurement of the curing characteristics

The curing characteristics of the NRF were obtained using an MDR (Rheoline, Mini MDR Lite) at the temperature of 150 °C. This was used to determine the torque, scorch time (t_{SI}) and curing time (t_{C90}), according to ASTM D5289.

2.4 Measurement of Mooney viscosity

The viscosity of the NRF was investigated by means of a Mooney viscometer, MV 3000 Basic (MonTech, Germany). The tests were performed at 100 °C using the large rotor, according to ASTM D1646.

2.5 Measurement of relative foam density and expansion ratio

The physical properties were investigated, including the relative foam density and expansion ratio. The relative foam density was measured according to ASTM D3575, using Equation 1 as given below:

$$\text{Relative foam density} = \frac{D_f}{D_c} \quad (1)$$

Where D_f is foam density (g/cm^3) and D_c (g/cm^3) is compound density.

The expansion ratio was calculated as the density of the NR compound specimen compared to the density of the natural rubber foam, as shown in Equation 2:

$$\text{Expansion ratio} = \frac{D_c}{D_f} \quad (2)$$

2.6 Measurement of hardness

The hardness of the NRF was measured in accordance with ASTM D2240 by using an indentation durometer

Table 2. Formulation of natural rubber compounds with different blowing agent contents and their mixing sequence and time.

Mixing sequence	Ingredients	Amount (phr)*	Mixing time (min)
1	NR	100	5
2	Stearic acid	1	1
3	ZnO	5	1
4	TMQ	1	1
5	CaCO ₃	30	3
6	TDAE oil	10	2
7	CBS	1	1
8	ADC	2, 4, 6, 8 & 10	1.5
9	Sulfur	2.5	1

*Part per hundred of rubber.

shore OO, and the readings were taken after a 10-second indentation. The compression-deflection of the NRF was determined according to ASTM D1056.

2.7 Measurement of compression-deflection before and after thermal ageing

Compression-deflection test was done according to ASTM D575. A sample with specimens approximately 12.5 mm thick and with a minimum area of 161 cm², was used for testing. The specimens were compressed between the parallel metal plates of the universal testing machine (Tinius Olsen, H10KS, Tinius Olsen Ltd., Surrey, UK) until the thickness reduced by 25%. The reading of the load was taken immediately. The test was repeated with the same specimen until the load readings did not change by more than 5%. For the compression-deflection change after oven ageing, similar test specimens were cut and placed in an oven for 168 h at a temperature of 70 °C. They were allowed to cool for at least 24 h and then the compression-deflection was determined. The percentage change in compression-deflection was calculated using Equation 3.

$$P = \left(\frac{A - O}{O} \right) \times 100 \quad (3)$$

Where P is the change in compression-deflection (%), O is the original compression-deflection and A is the final compression-deflection after oven ageing.

2.8 Compression set

Compression set was measured according to ASTM D395. A representative sample, approximately 12.5 mm thick and with a minimum area of 161 cm², was used for testing. The test specimens were compressed to 50% of their original thicknesses. The load was released after 22 h and the thickness was measured after 24 h at room temperature. The compression set calculation was as follows;

$$\text{Compression set (\%)} = \left[\frac{(t_0 - t_1)}{(t_0 - t_s)} \right] \times 100 \quad (4)$$

Where t₀ is the original thickness, t₁ is the thickness of the specimens after the specified recovery period and t_s is the thickness of the spacer bar used.

2.9 Swelling uptake

Swelling uptake was measured according to ASTM D471. Samples with dimensions of 25 × 50 × 6 mm³ were cut and weighed before and after immersion in toluene for 72 h under dark environment. It was preferable that the specimens were cut with clean, square edges. The swelling uptake was calculated as follows:

$$W = \left(\frac{A - B}{B} \right) \times 100 \quad (5)$$

Where W is the change in mass, A is the final mass of the specimen and B is the initial mass of the specimen.

2.10 Water absorption

Test specimens approximately 12.5 mm in thickness and 2500 mm² in area were used for this test. Round specimens were preferable. The specimens were submerged in distilled water below the water surface at room temperature for 3 min. The specimens were removed and blot dried. Then, the percentage change in mass was calculated based on the Equation 5.

2.11 Optical image and scanning electron microscopy

The physical appearance of NRF was captured using mobile phone camera through a default setting. While, the morphology was screened using a FEI Quanta™ 400 FEG scanning electron microscope (SEM; Thermo Fisher Scientific, Waltham, Massachusetts, USA). Each specimen was coated with a layer of gold/palladium to remove the charges that had built up during imaging.

3. Results and Discussion

3.1 Mooney viscosity

Figure 1 shows the Mooney viscosity of the NRF prepared using various levels of ADC content. The Mooney viscosity is a measure of the flow properties of the rubber^[12,13]. This correlates well with the processability of rubber foam, since lower viscosity enables the easy diffusion of the gas phase while foaming during vulcanisation. It can be seen that the Mooney viscosity of the rubber compounds increased with the addition of ADC. ADC is rigid in nature, so it may reduce deformable parts and restrict the movement of rubber molecules. It was noted that the tested temperature was 100 °C, which is lower than the decomposition temperature of ADC (approximately 150 °C). Therefore, no bubbles occurred while measuring the Mooney viscosity.

3.2 Curing characteristics

The rheometric curves of the NRF produced by varied levels of blowing agent content are shown in Figure 2, while the data extracted from the curves are summarised in Table 3. It was found that the maximum torque (M_H) increased after adding the ADC, showing that the material

is stiffer over the addition of ADC. This can be explained from the increase in delta torque ($M_H - M_L$) as the torque difference is an indirect indication of extent of cross-link^[14]. The scorch time (t_{SI}) and curing time (t_{C90}) increased with

Table 3. Cure characteristics of NRF prepared by various ADC content.

ADC Content (phr)	M_H (dNm)	M_L (dNm)	$M_H - M_L$ (dNm)	t_{SI} (min)	t_{C90} (min)	CRI (min ⁻¹)
2	20.6	1.38	19.19	1.84	12.14	9.71
4	24.5	1.52	22.97	2.14	13.77	8.60
6	28.7	1.58	27.12	2.35	15.48	7.62
8	32.9	2.03	30.89	2.35	15.72	7.48
10	31.3	1.25	30.00	2.31	15.18	7.77

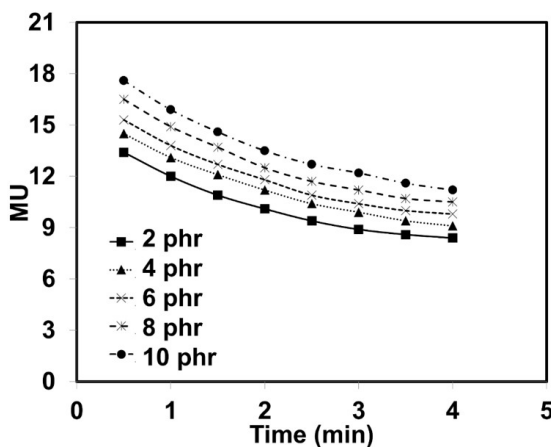


Figure 1. Mooney viscosity of NRF prepared by various ADC content.

the addition of ADC. t_{SI} is the induction time experienced by a rubber compound before vulcanisation is initiated, while t_{C90} is the time rubber takes to become 90% vulcanised. The increase in these two values indicated that ADC can prolong the vulcanisation time of rubber due to its action as a blowing agent. It tended to generate the gas phase while heating and delay the action of the vulcanising accelerator while curing. Another possible reason may be the action of the ADC after chemical decomposition^[15].

According to Harpell et al.^[16] and Bhatti et al.^[17], the decomposition of ADC goes through competitive and exothermic reaction pathways, as shown in Figure 2, producing hydraazodicarbonamide, urazol and a gaseous mixture of nitrogen (N_2), carbon monoxide (CO), cyanic acid (HNCO) and ammonia (NH_3). N_2 is the main source of gas that make the foam free flowing. Different paths may be favored over other depending on the process conditions and the state of the product. The focal point here is the production of cyanic acid, which is acidic in nature. An increase in cyanic acid is particle size-dependent. As reported by Reyes-Labarta and Marcilla^[15], when the ADC particle size increases, the reaction rate of this heterogeneous reaction may increase due to the longer contact time between the cyanic acid gas (produced from reactions i and ii) and the ADC particles. Consequently, there may be a probability that the cyanic acid gas will react with the unreacted ADC, through reaction iii, thus accelerating the degradation process. Any chemical substance that makes a rubber compound more acidic will cause the adsorption of accelerators^[18] and retard their reactivity. This makes the vulcanising process longer when ADC is added to the rubber compounds.

3.3 Physical properties

Table 4 lists the relative foam densities and expansion ratios of the NRF with different levels of ADC content.

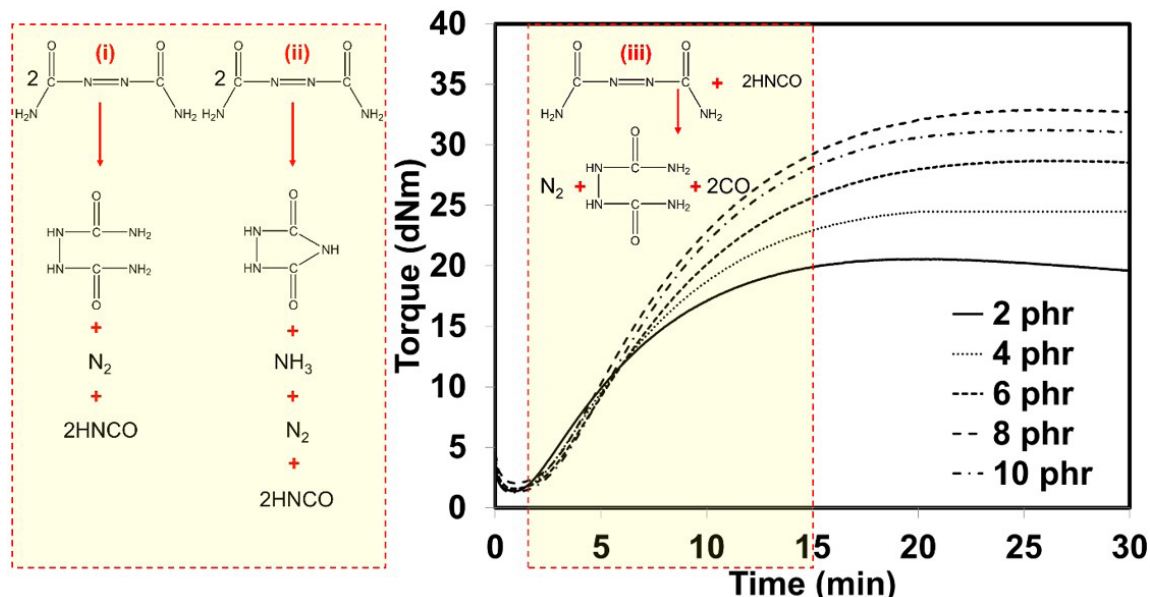


Figure 2. Chemical decomposition of ADC and rheometric curves of NRF prepared by various ADC content (The reaction schemes were adapted from Reyes-Labarta and Marcilla^[15]).

As greater concentrations of the blowing agent were used, more gas was subsequently generated. This reduced the relative foam density, which significantly decreased from 0.78 g/cm^3 to 0.46 g/cm^3 . Higher ADC concentrations shortened the growth time of the foam, thus restricting the escape of gas through the foam surface. This allowed the foam to expand more and, consequently, produce foam with a lower relative density^[19]. The relative foam density was directly related to the porosity values and expansion ratio because the high amount of gas trapped in the matrix occurred due to the large size of the NRF specimens. For this reason, the low relative foam density when high amounts of ADC were used revealed the considerable expansion of these NRF specimens. The porosity values and expansion ratios are shown in Table 4. The decrease in relative foam density also played a role by increasing the number of cells per unit volume. Figure 3 shows that as the blowing agent concentration increased, the number of cells per unit volume also increased. This was the case except for the sample at 10 phr of ADC. As more gas was produced due to the higher ADC content, this indicated more efficient gas production. The cell sizes grew due to the destruction of the cell walls.

Table 4 also lists the hardness and compression set of the NRF prepared using various levels of ADC content. The hardness decreased with an increase in the ADC content. This was due to the higher foam porosity in the NR matrix during the formation of the gas phase. The compression set of the foams was also studied to determine the recovery properties of a sample after it had been subjected to a constant deflection for a specified time/temperature/deflection by measuring its gauge before and after the test period. The compression set of the specimens was higher with the addition of ADC content. A lower compression set indicates better recovery after constant deflection. The compression set correlated well with the elastic response of the rubber in association with the crosslink density of the sample^[20]. Increasing levels of ADC caused more porosity in the foam. This happened with the increment in the cell size and the reduction of the cell wall per surface area. Cell walls mainly control the elastic response due to their elastic phase. Different cell sizes and cell numbers appeared to critically affect the compression set values.

Further evidence can be identified from the SEM images shown in Figure 3. The SEM images show that a systematic correlation between the number of cells per unit volume

Table 4. Relative foam density, expansion ratio, hardness and compression set of NRF prepared by various ADC content.

ADC Content (phr)	Relative Foam Density (RFD)	Expansion Ratio	Porosity (1 – RFD)	Hardness (Shore OO)	Compression Set (%)
2	0.78 ± 0.05	1.28 ± 0.05	0.22	65 ± 0.29	1.29 ± 0.45
4	0.61 ± 0.02	1.63 ± 0.02	0.39	64 ± 0.54	1.52 ± 0.43
6	0.58 ± 0.02	1.73 ± 0.02	0.42	60 ± 1.23	2.01 ± 0.43
8	0.55 ± 0.02	1.82 ± 0.02	0.45	58 ± 0.91	2.05 ± 0.43
10	0.46 ± 0.01	2.18 ± 0.01	0.54	56 ± 0.79	2.17 ± 0.46

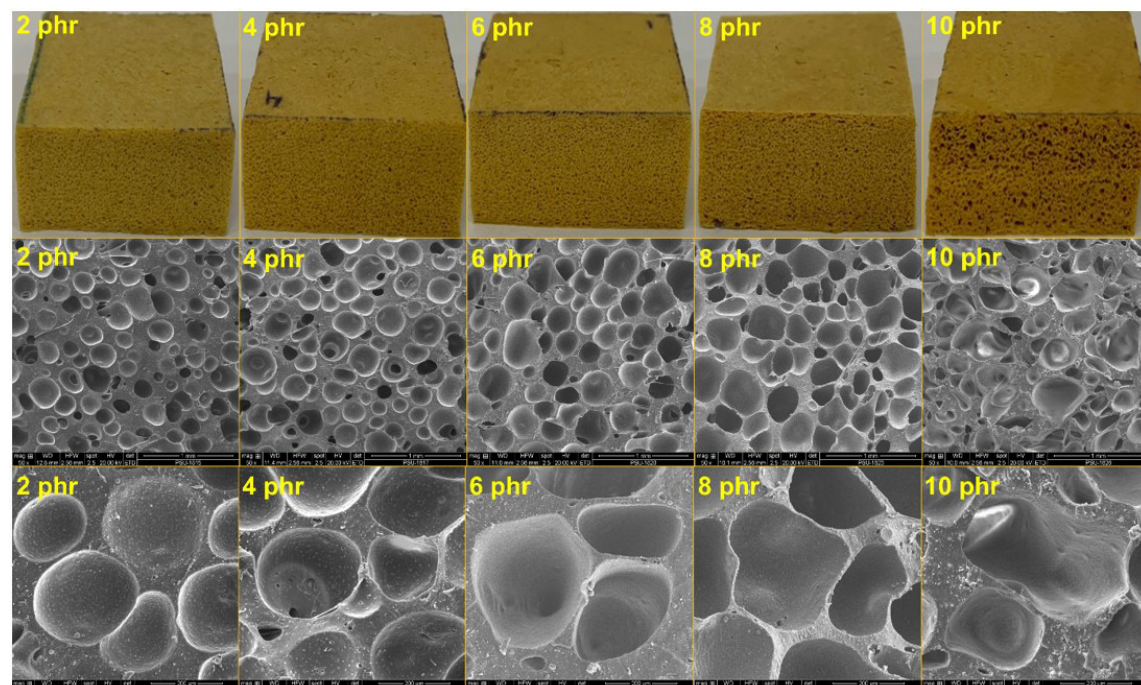


Figure 3. Optical image (top) and SEM images at 50× (middle) and 300× (bottom) magnifications of NRF prepared by various ADC content.

and the average cell size. An increase in the blowing agent concentration resulted in smaller, finer and more uniform cells. The decomposition of high concentrations of nitrogen gas occurred simultaneously for a given time, so more cells formed at that particular time. Consequently, the number of cells per unit volume increased, resulting in a smaller average cell size in the foam^[9]. This phenomenon was found in reverse for the ADC sample at 10 phr. This was because of the weakness of the cell walls due to the diffusion of gas from one cell to another, which broke the cell walls and led to larger cell sizes at this amount. The SEM images are in good agreement with the porosity values and expansion ratios reported in the previous section.

3.4 Swelling uptake and water absorption

The swelling uptake values of the NRF were also measured in this study (see Figure 4a). The swelling percentage was investigated by toluene uptake until equilibrium swelling was reached at room temperature. Adding more ADC caused the swelling uptake of the rubber foam to increase. As mentioned previously, the number of cells increased and the thickness of cell walls reduced when higher amounts of ADC were used. As the number of cells and the cell size increased, the porosity increased (see Table 4), the solvent could penetrate more easily from one cell to another, leading

eventually to an increase in the swelling uptake. This would increase the swelling uptake.

As highlighted in the introduction, the main focus of this study was to classify the rubber foam grade that met the basic requirements, according to ASTM D1056. From this section onwards, the required properties are presented and discussed. Firstly, the water absorption of the rubber foam will be discussed (see Figure 4b). The water absorption was used to distinguish the cell structure of the prepared foam^[21]. Higher absorption of water in the sample indicated the foam had a more open-cell structure. As for the closed-cell structure of the foam, the classification of foam depends on the relative foam density of the rubber foam. Referring to Table 1 and the relative foam densities listed in Table 3, the water absorption of rubber foam should be less or equal to 5%. Hence, it was concluded that the water absorption of the rubber foam met the standard requirements, regardless of ADC content. The next steps were to consider other factors in order to classify the grade number of the rubber foam.

3.5 Compression-deflection before and after thermal ageing and foam classification

Figure 5a shows the compression-deflection values of the NRF prepared with various levels of ADC content. It was observed that the compression-deflection decreased

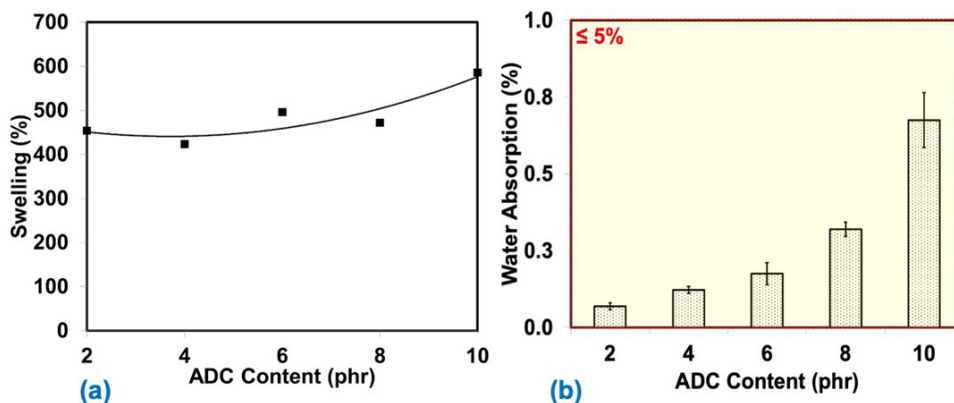


Figure 4. Swelling uptake (a) and water absorption (b) of NRF prepared by various ADC content.

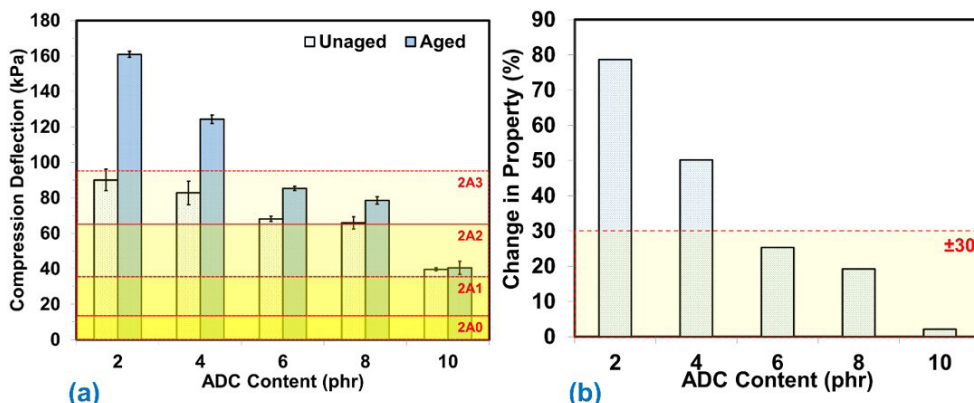


Figure 5. Compression-deflection before and after thermal aging (a) and their corresponding change in property (b) of NRF prepared by various ADC content.

with the inclusion of ADC. Low compression-deflection values indicated the poor ability of the NRF to take on external forces^[22]. Increasing the ADC content caused a high amount of gas to be produced in the rubber matrix. It also definitely increased the number of cells, resulting in weaker cell walls and reductions in foam stress. The compression-deflection values agreed well with the SEM images shown in the previous section. The compression-deflection values before thermal ageing were implemented to further classify the foam grades. Each grade is based on a specific firmness range, which is expressed by compression-deflection. The grades are designated by digit, the softer grades being identified with lower numbers and the higher grades being identified with higher numbers. Here, it was observed that the compression-deflection values were grouped as 2A3, except for the sample containing 10 phr of ADC, which was 2A2. When these samples were placed under severe thermal treatment, the values were higher than those of the unaged samples. This was due to the hardened characteristics of the foam due to the increase in modulus caused by the radical recombination of chain scission.

The values before and after ageing were then calculated for the changes in property, which can be seen in Figure 5b. The property changes were reduced with the addition of ADC. Lower values indicate the higher thermal stability of rubber vulcanisate^[23,24]. Increasing the amount of ADC reduced the cell wall thickness due to the increased porosity. The rubber phase was then reduced, which led to a reduction in the crosslinking site in the rubber. The thermal stability finally increased with the addition of ADC. In addition to this, property changes were also used to classify foam grades. As shown in Table 1, the ASTM D1056 requirement is that this value should not exceed 30%. The results indicated that the ADC content from 6 – 10 phr met the standard requirements. Based on the overall findings, the addition of this level of ADC content was suitable for the preparation of NRF. However, the cell morphology should also be considered because rubber foams depend greatly on this. From the optical images, together with the SEM images (see Figure 3), it was clear that the ADC content at 6 phr produced a homogeneous cell size and cell wall distribution.

4. Conclusion

This study focused on the classification of NRF grades by varying the content of a blowing agent. The foams were classified based on the basic properties required by ASTM D1056. In this study, different blowing agent concentrations (2, 4, 6, 8, and 10 phr) were shown to influence the curing properties of NRF. Increased ADC content resulted in a lower relative foam density and larger porosity value and expansion ratio. It was also found that the hardness and compression-deflection of the NRF decreased noticeably with increased ADC content. This was due to the increase in the gas phase raised by the ADC. The addition of ADC lengthened the scorch (t_{s1}) and curing times (t_{c90}) of the foam. Furthermore, the hardness and compression-deflection decreased with the inclusion of ADC, since these values were higher after oven ageing due to the radical recombination caused by chain breaking. According to ASTM D1056, the compression-deflection values of the prepared foams were the 2A2 and

2A3 grades, while the ADC content at 6 – 10 phr met the basic properties required by the same standard. Furthermore, the ADC content at 6 phr was strongly suggested, in terms of the morphology of the foam. This showed the homogeneous cell size and cell wall distribution. The results obtained from this study will provide useful information when preparing NRF that meets the basic properties stated in ASTM D1056.

5. Author's Contribution

- **Conceptualization** – Fateehah Baru; Sitisaiyidah Saiwari; Nabil Hayeemasae.
- **Data curation** – Fateehah Baru; Nabil Hayeemasae.
- **Formal analysis** – Fateehah Baru; Nabil Hayeemasae.
- **Investigation** – Fateehah Baru.
- **Methodology** – Sitisaiyidah Saiwari; Nabil Hayeemasae.
- **Project administration** – Nabil Hayeemasae.
- **Resources** – Nabil Hayeemasae.
- **Software** – Nabil Hayeemasae.
- **Supervision** – Sitisaiyidah Saiwari; Nabil Hayeemasae.
- **Validation** – Nabil Hayeemasae.
- **Visualization** – Nabil Hayeemasae.
- **Writing – original draft** – Nabil Hayeemasae.
- **Writing – review & editing** – Sitisaiyidah Saiwari; Nabil Hayeemasae.

6. Acknowledgements

We gratefully acknowledge the financial support by Natural Rubber Innovation Research Institute, Prince of Songkla University through the Grant No. SAT6201175S. The first author wishes to thank the Faculty of Science and Technology, Prince of Songkla University, Pattani Campus for providing a personal scholarship through the Grant No. 005/2562.

7. References

1. Toncheva, A., Brison, L., Dubois, P., & Laoutid, F. (2021). Recycled tire rubber in additive manufacturing: selective laser sintering for polymer-ground rubber composites. *Applied Sciences (Basel, Switzerland)*, 11(18), 8778. <http://dx.doi.org/10.3390/app11188778>.
2. Mutlu, İ., Sugözü, İ., & Keskin, A. (2015). The effects of porosity on friction performance of brake pad using waste tire dust. *Polímeros: Ciéncia e Técnologia*, 25(5), 440-446. <http://dx.doi.org/10.1590/0104-1428.1860>.
3. Suethao, S., Phongphanphanee, S., Wong-ekkabut, J., & Smithipong, W. (2021). The relationship between the morphology and elasticity of natural rubber foam based on the concentration of the chemical blowing agent. *Polymers*, 13(7), 1091. <http://dx.doi.org/10.3390/polym13071091>. PMid:33808133.
4. Najib, N. N., Ariff, Z. M., Bakar, A. A., & Sipaut, C. S. (2011). Correlation between the acoustic and dynamic mechanical properties of natural rubber foam: effect of foaming temperature. *Materials & Design*, 32(2), 505-511. <http://dx.doi.org/10.1016/j.matdes.2010.08.030>.
5. Ramasamy, S., Ismail, H., & Munusamy, Y. (2013). Effect of rice husk powder on compression behavior and thermal

- stability of natural rubber latex foam. *BioResources*, 8(3), 4258-4269. <http://dx.doi.org/10.15376/biores.8.3.4258-4269>.
- Panploo, K., Chalermisinsuwan, B., & Poompradub, S. (2019). Natural rubber latex foam with particulate fillers for carbon dioxide adsorption and regeneration. *RSC Advances*, 9(50), 28916-28923. <http://dx.doi.org/10.1039/C9RA06000F>. PMid:35528441.
 - Ariff, Z. M., Zakaria, Z., Tay, L. H., & Lee, S. Y. (2007). Effect of foaming temperature and rubber grades on properties of natural rubber foams. *Journal of Applied Polymer Science*, 107(4), 2531-2538. <http://dx.doi.org/10.1002/app.27375>.
 - Pechurai, W., Muansupan, T., & Seawlee, P. (2014). Effect of foaming temperature and blowing agent content on cure characteristics, mechanical and morphological properties of natural rubber foams. *Advanced Materials Research*, 844, 454-457. <https://doi.org/10.4028/www.scientific.net/AMR.844.454>.
 - Charoeythornkhajornchai, P., Samthong, C., Boonkerd, K., & Somwangthanaroj, A. (2016). Effect of azodicarbonamide on microstructure, cure kinetics and physical properties of natural rubber foam. *Journal of Cellular Plastics*, 53(3), 287-303. <http://dx.doi.org/10.1177/0021955X16652101>.
 - Lee, E.-K., & Choi, S.-Y. (2007). Preparation and characterization of natural rubber foams: effects of foaming temperature and carbon black content. *Korean Journal of Chemical Engineering*, 24(6), 1070-1075. <http://dx.doi.org/10.1007/s11814-007-0123-6>.
 - Yang, H.-H., & Han, C. D. (1984). The effect of nucleating agents on the foam extrusion characteristics. *Journal of Applied Polymer Science*, 29(12), 4465-4470. <http://dx.doi.org/10.1002/app.1984.070291281>.
 - Ehabé, E., Bonfils, F., Aymard, C., Akinlabi, A. K., & Sainte Beuve, J. (2005). Modelling of Mooney viscosity relaxation in natural rubber. *Polymer Testing*, 24(5), 620-627. <http://dx.doi.org/10.1016/j.polymertesting.2005.03.006>.
 - Kramer, O., & Good, W. R. (1972). Correlating Mooney viscosity to average molecular weight. *Journal of Applied Polymer Science*, 16(10), 2677-2684. <http://dx.doi.org/10.1002/app.1972.070161020>.
 - Ismail, H., & Anuar, H. (2000). Palm oil fatty acid as an activator in carbon black filled natural rubber compounds: dynamic properties, curing characteristics, reversion and fatigue studies. *Polymer Testing*, 19(3), 349-359. [http://dx.doi.org/10.1016/S0142-9418\(98\)00102-0](http://dx.doi.org/10.1016/S0142-9418(98)00102-0).
 - Reyes-Labarta, J. A., & Marcilla, A. (2007). Kinetic study of the decompositions involved in the thermal degradation of commercial azodicarbonamide. *Journal of Applied Polymer Science*, 107(1), 339-346. <http://dx.doi.org/10.1002/app.26922>.
 - Harpell, G. A., Gallagher, R. B., & Novits, M. F. (1977). Use of azo foaming agents to produce reinforced elastomeric foams. *Rubber Chemistry and Technology*, 50(4), 678-687. <http://dx.doi.org/10.5254/1.3535165>.
 - Bhatti, A. S., Dollimore, D., Goddard, R. J., & O'Donnell, G. (1984). The thermal decomposition of azodicarbonamide. *Thermochimica Acta*, 76(1-2), 63-77. [http://dx.doi.org/10.1016/0040-6031\(84\)87004-5](http://dx.doi.org/10.1016/0040-6031(84)87004-5).
 - Ballard, D. G. H., Myatt, J., & Richter, J. F. P. Some observations on the mechanism of action of retarders in rubber vulcanization. A new class of retarder. *Journal of Applied Polymer Science*, 16(10), 2647-2655. <http://dx.doi.org/10.1002/app.1972.070161017>.
 - Guan, L. T., Du, F. G., Wang, G. Z., Chen, Y. K., Xiao, M., Wang, S. J., & Meng, Y. Z. (2007). Foaming and chain extension of completely biodegradable poly(propylene carbonate) using DPT as blowing agent. *Journal of Polymer Research*, 14(3), 245-251. <http://dx.doi.org/10.1007/s10965-007-9103-0>.
 - Yamsaengsung, W., & Sombatsompop, N. (2009). Effect of chemical blowing agent on cell structure and mechanical properties of EPDM foam, and peel strength and thermal conductivity of wood/NR composite-EPDM foam laminates. *Composites. Part B, Engineering*, 40(7), 594-600. <http://dx.doi.org/10.1016/j.compositesb.2009.04.003>.
 - Zhang, G., Wu, Y., Chen, W., Han, D., Lin, X., Xu, G., & Zhang, Q. (2019). Open-cell rigid polyurethane foams from peanut shell-derived polyols prepared under different post-processing conditions. *Polymers*, 11(9), 1392. <http://dx.doi.org/10.3390/polym11091392>. PMid:31450807.
 - Azevedo, J. B., Chávez, M. A., & Rabello, M. S. (2011). Efeito de reticulante na morfologia e propriedades fisicomecânicas de espumas poliméricas obtidas com EVA e EPDM. *Polímeros*, 20(5), 407-414. <http://dx.doi.org/10.1590/S0104-14282011005000002>.
 - Motice, F., & Bigdeli, T. (2020). Prediction of mechanical and functional features of aged rubber composites based on BR/SBR; structure-properties correlation. *Materials Research*, 22(6), e20190226. <http://dx.doi.org/10.1590/1980-5373-mm-2019-0226>.
 - Hayeemasae, N., & Masa, A. (2020). Relationship between stress relaxation behavior and thermal stability of natural rubber vulcanizates. *Polímeros: Ciéncia e Tecnologia*, 30(2), e2020016. <http://dx.doi.org/10.1590/0104-1428.03120>.

*Received: Jan. 01, 2022**Revised: Apr. 10, 2022**Accepted: May 19, 2022*